High-resolution optical spectroscopy of nickel ions in II-VI semiconductors: Isotope shifts at the $^3T_1(F)\leftrightarrow{}^3T_1(P)$ and $^3T_1(F)\leftrightarrow{}^3A_2(F)$ Ni^{2+} transitions in CdS and ZnS crystals

I. Broser, A. Hoffmann, and R. Germer

Institut für Festkörperphysik II der Technischen Universität Berlin, D-1000 Berlin 12, Germany

R. Broser and E. Birkicht

Fritz-Haber-Institut der Max-Planck-Gesellschaft, D-1000 Berlin-Dahlem 33, Germany

Extremely narrow fine structures in the absorption, emission, and excitation spectra of the Ni^{2+} transitions $^3T_1(F)\leftrightarrow{}^3T_1(P)$ and $^3T_1(F)\leftrightarrow{}^3A_2(F)$ have been achieved by doping CdS and ZnS crystals with very small concentrations of nickel impurities. The incorporation of up to five different nickel isotopes leads to the appearance of clearly resolved isotope splittings of the lines. For the first time the dependence of such splittings on different transitions, different second neighbors, and on external parameters—such as the magnetic field, uniaxial stress, and temperature—has been measured. An adequate description of the assumed level structure and the isotope effect can be obtained by considering the influence of the local phonon energy and of the Jahn-Teller effect for both the initial and the final states of the transitions considered.

I. INTRODUCTION

The positions of the energy levels of ions, incorporated into a solid, are strongly influenced by the surrounding host lattice. Transitions between such energy levels give rise to absorption[1,2] and emission[3] spectral lines and bands, which normally are considerably broadened, compared to those observed in a free ion. This is a consequence of shifts and splittings by the static crystal field and by lattice vibrations. The analysis of the spectra then becomes difficult as in most spectroscopic experiments, only the observed fine structures allow an unambiguous coordination of spectral lines to a particular transition within a theoretically developed energy scheme. This holds also for the action of external influences, like magnetic, electric, or stress fields. Progress in the spectroscopy of impurity ions in solids is therefore markedly linked with progress in the preparation of highly resolved structures in the spectra.

It has been reported, that nickel ions incorporated into broadband II-VI and III-V semiconductors lead in some cases to the appearance of exceptionally narrow lines in absorption,[4-7] emission,[8-10] and excitation[11,12] so that new structures could be detected. Therefore, nickel seems to be an ideal atom, not only to understand its energy scheme, but also to study the ideal and real structures of the host lattice. Isotope effects, zero field splittings, ion-ion interactions, static and dynamic Jahn-Teller interactions can thus be investigated as well as very small shifts and splittings of the lines by temperature, stress, electric, and magnetic fields. New and unexpected effects become visible.

First, we aim at showing the experimental conditions, under which extremely narrow spectral structures of nickel atoms can be achieved, and at understanding the partic-ular incorporation mechanism in a II-VI host lattice. Second, we report on results, using high-resolution optical spectroscopy, which allow us to understand the fine structures of the spectra within the scope of existing energy models, taking into account crystal-field effects as well as electron-phonon interactions.

We mainly intended to study and explain a particular fine structure, the splitting of lines for different nickel isotopes in the two broad energy gap semiconductors ZnS and CdS. Isotope effects are strongly connected with lattice vibrations and are therefore a means to understand vibronic effects due to electron-phonon interactions.[13-15] As these phenomena are often responsible for strong deviations of the real energy scheme from the simple static crystal-field approximation, studying isotope splittings is an important tool to separate pure electronic from phononic influences. For the first time it has been observed that isotope splitting energies are different for different transitions in the same ion and that they can be changed by applying stress, magnetic fields, or different temperatures.

II. EXPERIMENTS

A. Preparation of crystal specimen for high-resolution spectroscopy

Investigating fine structures in the optical spectra of impurities in solids demands highly perfect crystals. II-VI semiconductors particularly CdS and ZnS crystals are produced with a minimum of lattice defects (dislocations, vacancies, etc.) and the disturbing impurities are kept extremely low by using the Frerichs-Warminsky[16] method: Thin platelets as well as pencil-shaped rods are formed through vapor transport by sublimation of the polycrys-

talline compound. Good crystals have been demonstrated to show the effect of anomalous x-ray absorption[17] due to a very small amount of dislocations. While all CdS crystals crystallize to the hexagonal modification, the ZnS crystals are preferably cubic with stacking faults of the H4 and H8 polytypic structure.

To get narrow spectral lines, small concentrations of the nickel ions are necessary. This has been concluded from measurements with not intentionally doped CdS crystals,[18] but it was not possible to measure the nickel concentration of these crystals. Clear evidence of nickel ions and their concentration could be achieved by doping the crystals with isotopes ^{61}Ni, ^{62}Ni, and ^{64}Ni, which exist in the natural element in the order of a few percent[19] only.

By evaporation selected CdS and ZnS crystals have been covered with a measurable amount of doping material. The virtual average thickness of the Ni layers varied between 0.02 and 2 nm, the number of doping atoms at the crystal surface was therefore $10^{12}-10^{14}$ cm^{-2}. Following the evaporation process, the crystals were annealed for about 2 hours at a temperature of 800°C in small evacuated quartz ampoules. In some cases a certain amount of sulfur or cadmium was added.

Figure 1 shows the doping effect for the zero phonon lines of the crystal field transition $^3T_1(F) \rightarrow {}^3T_1(P)$ of Ni^{2+} in CdS. The higher doped crystal (CdS B349 with 1,5 nm Ni) has a half-width about 10 times greater than crystal B354 with 0,1 nm Ni. Our example shows that a broadening of the linewidth by Ni^{2+}-Ni^{2+} interactions occurs already at relatively low concentrations. As the higher doped crystal B349 contains only 1 ppm Ni atoms, for high-resolution spectroscopy, therefore, Ni^{2+} concentrations of some 10^{-2} ppm are needed.

It should be mentioned that only the concentration of Ni^{2+} ions counts. This has been demonstrated by annealing crystals with the same Ni concentration in a cadmium or sulfur atmosphere, respectively. Cadmium in excess creates small narrow lines, while sulfur in excess gives rise
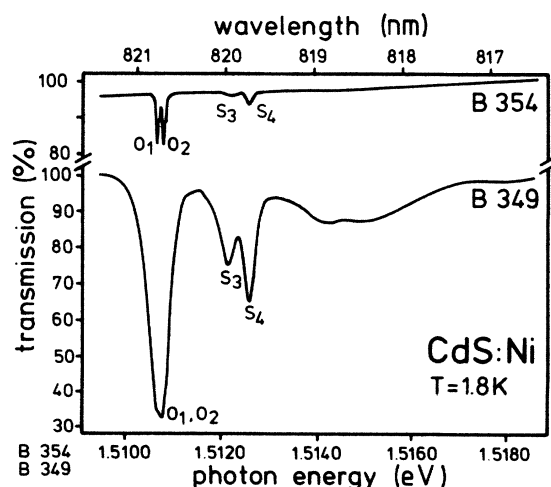

FIG. 1. Unpolarized transmission spectra of two CdS crystals doped with different amounts of Ni ions and annealed in a cadmium (B354) and a sulfur (B349) atmosphere, respectively. Evaporated Ni layer: CdS B354: 0,1 nm, CdS B349: 1,2 nm /35/.
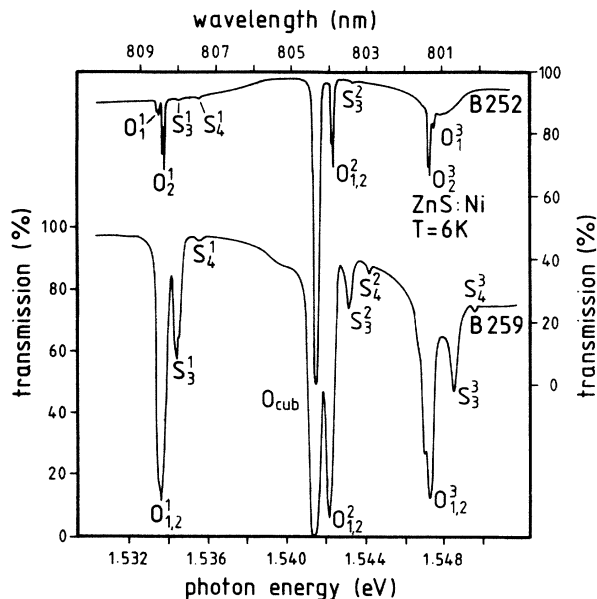

FIG. 2. Unpolarized transmission spectra of two ZnS crystals doped with different amounts of Ni ions and annealed both in sulfur atmosphere. Evaporated Ni layer: ZnS B252: 1 nm, ZnS B259: 20 nm. The scale on the right is valid for ZnS B259, on the left for ZnS B252.

to big broad lines. In the first case, n-type material is produced changing the majority of the Ni-atoms into the "inactive" Ni^+ state. In the second case, sulfur lowers the Fermi level so that most of the Ni atoms are in the Ni^{2+} state, responsible for the observed spectra.

A corresponding impressive example showing the influence of doping for ZnS-Ni^{2+} is given in Fig. 2. Here the doping concentration had the ratio $a:b = 1:20$. A sulfur atmosphere was applied in both cases during the annealing. It can clearly be seen that the polarized spectra of crystal ZnS B252 show extremely narrow lines, while the crystal ZnS B259 containing much more Ni shows much broader lines. This is also true for lines with equal values for the transmission minima.

To sum up, it has been demonstrated that CdS and ZnS crystals doped with different Ni isotopes can be produced, having absorption lines with an extremely small half-width lower than 50 μeV. Similar values have been observed for emission and excitation spectra, therefore high-resolution spectroscopy becomes possible to investigate fine structures.

B. Zero-phonon absorption, emission, and excitation lines

No doubt, the transmission spectra, shown in Figs. 1 and 2, are connected with transitions within the d-shell of Ni^{2+} substituting CdS, respectively, ZnS lattice sites. From the literature[1-12] it is known that for these two compounds a Ni^{2+} ion in a tetrahedral configuration including spin-orbit coupling with four sulfur atoms as next neighbors gives rise to transitions near 800 nm, starting—due to the static crystal-field theory—at the lowest A_1 level of the $^3T_1(F)$ term and having its final

state at the lowest E and T_2 level of the $^3T_1(P)$ term (see first three columns of Fig. 3). Convincing arguments[5] exist that the two higher levels of the $^3T_1(P)$ term, split by spin-orbit interaction, T_1 and A_1, are not involved in our experiments, as they are expected to give rise to transitions far away in energy from the spectral region under consideration. In a cubic crystal, like ZnS zinc blende, one expects just one absorption line, due to the fact that a transition from an A_1 to an E level is dipole forbidden. For the hexagonal wurtzite structure of CdS and ZnS and for polytypes of ZnS, the T_2 level splits into an A_1 and an E term, so that three lines should be observed, two of them polarized perpendicular and one parallel to the c axis. As we see from Figs. 1 and 2, however, at least four zero-phonon lines exist for CdS and for each spectral group in ZnS. Attempts have been made to explain this puzzle by including additional levels in the energy scheme originating from quantized vibrations of the Ni ion[5,6] (see 4th column of Fig. 3). Strong electron-phonon interactions such as the Jahn-Teller effect will then alter the energy scheme for zero-phonon transitions entirely, not only allowing us to understand the number of possible transitions, but also the existence and strength of an isotope effect (see 5th column of Fig. 3). Up to now, however, a quantitative agreement of theory and experiment could not be given. This might be due to theoretical problems, attested to by the widely diverse basic assumptions of the different authors.[1,5,6,20] Clearly it was also due to an existing lack of experimental details on the fine structure of the spectra under varying conditions. It is the aim of this paper, by using the high-quality specimen described above, to provide a substantial amount of new informa-

tion, essential to the understanding of the mechanism of the electron-phonon interaction and its influence on the vibronic energy scheme. In Fig. 3 our arguments given below in the discussion are already taken into consideration.

An important means to study optical transitions in solids is the investigation of excitation spectra of emission lines. The existence of radiant transitions is a necessity here. For the first time such luminescence spectra, partly coinciding with the transmission spectra, could be detected for CdS-Ni and ZnS-Ni in our laboratory.

Figure 4 compares transmission, emission, and excitation spectra for CdS in the region of the $^3T_1(F) \leftrightarrow ^3T_1(P)$ transition. Crystals with relatively high nickel concentrations, giving rise to broader lines, enable us to measure the emission and excitation spectra. Nevertheless, these experiments produced new information. First of all, only for two lines (called O_1 and O_2 in Fig. 1), absorption and emission overlap. No doubt, the corresponding transitions take place between the ground levels of the $^3T(F)$ and $^3T_1(P)$ terms. The origin of the high-energy absorption and the low-energy emission lines is not that easy to explain and needs further investigations. From the excitation spectrum of the low-energy emission line, however, it becomes evident that all the lines are due to transitions within the same center. Any possible energy scheme, therefore, has to include all the observed structures. From the isotope effect, described in the next section, it is also obvious that nickel is the impurity in question.

A similar comparison between transmission and emission spectra is demonstrated for polytypic ZnS-Ni crystals in Fig. 5. The spectra consist of three groups of lines for which both optical processes, luminescence, and absorption, coincide in the energy positions. At lower wavelengths the emission spectrum additionally shows a variety of lines placed onto a broad band. It is very likely that the high-energy lines are zero-phonon lines due to transitions within nickel centers at three or four different polytypic surroundings. Furthermore, obviously three groups of low-energy emission lines exist with an almost
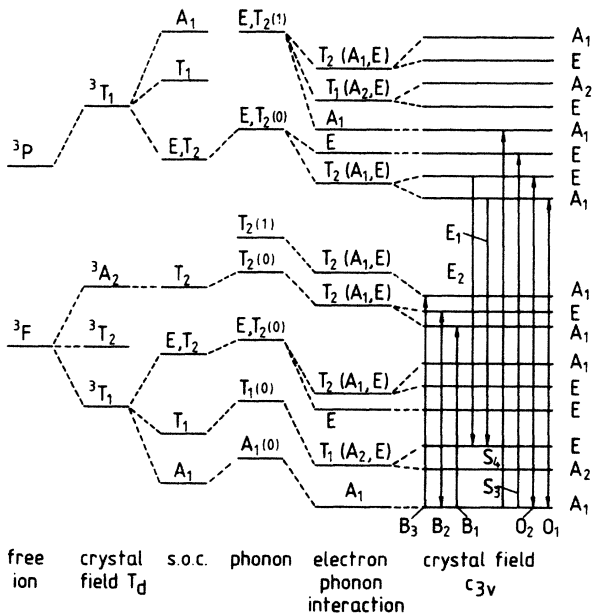

FIG. 3. Energy scheme showing the levels of the free ion, split and shifted by cubic crystal field, spin orbit coupling, phonon ladder, electron-phonon interaction, and a trigonal crystal field. The main transitions, observed in this paper are indicated by arrows. Transition between A_1 states is polarized $E||c$, between A_1 and E states $E\perp c$, transition E_2 between E states is almost unpolarized (see Fig. 7).
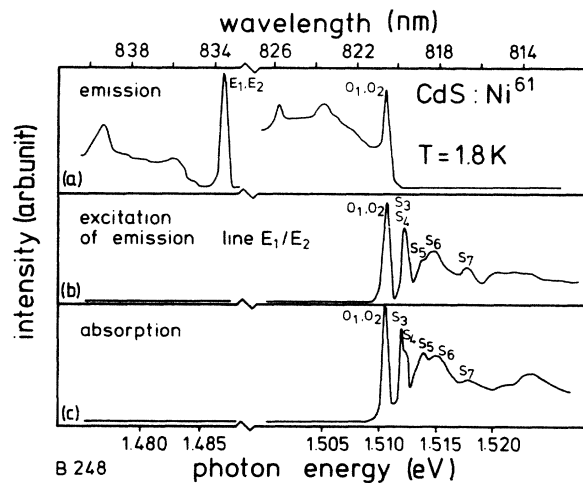

FIG. 4. Unpolarized emission, excitation and absorption spectra of a heavily doped CdS crystal. Light source for emission and excitation: Tunable excimer laser.
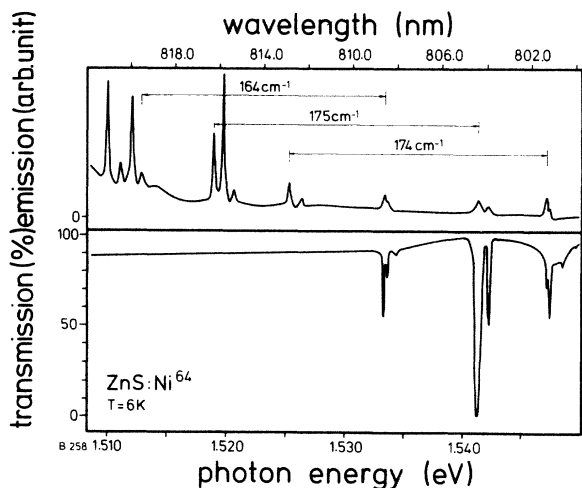
FIG. 5. Unpolarized emission and transmission spectra of a ZnS polytypic crystal with medium ^{64}Ni doping and sulfur vapor annealing. Light source for emission: cw Argon laser.

equal energetic distance of about 170 cm^{-1} to the high-energy groups. Compared with Fig. 4 it becomes evident that they will have the same origin as the E lines in CdS. The additional line structure of the emission spectrum shown in Fig. 5 at longer wavelengths than 820 nm is the beginning of a many-line structure and has been connected earlier with the M centers;[21,22] it shows up in varying intensities in almost all investigated Ni-doped ZnS polytypes, so that a relationship to the $3d$ transitions is evident. The problem is, however, not relevant in connection with the subject dealt with here, and will therefore be discussed elsewhere.

It is known that ZnS (Ref. 20) and CdS (Ref. 21) crystals doped with Ni centers, also show optical transitions in the near-infrared region at 1,1 to 1,3 μm. They have been connected with transitions within the ^3F term. For the

first time we could observe them also as luminescent transitions. Of major importance was the fact that very large isotope splittings were detected in these spectra. In this section the infrared $^3T_1(F)\leftrightarrow{}^3A_2(F)$ transitions for CdS-Ni in absorption and emission are presented for just one Ni isotope (Fig. 6). Again a zero-phonon doublet (B_2,B_3) can be seen, where emission and absorption overlap, and some additional structure becomes visible on both sides of this overlap. The interpretation is, as we will see, similar to that of the lines around 820 nm.

C. The isotope effect

As already stated above, a comparison of our experiments with the usual energy scheme of a nickel impurity in a static lattice with tetrahedral[1] or trigonal[18] coordination gives no satisfactory agreement. Vibronic effects like the Jahn-Teller effect have to be included and additional experiments are necessary. Such experiments should change in a reproducible and continuous way the conditions under which the electron-phonon interaction occurs. One way, already described above, is to study the influence of different host lattices (CdS,ZnS), of the structure (hexagonal, polytypic cubic, etc.), or of the initial or final states of the transition. Another possibility is to vary the mass of the impurity itself and to observe isotope shifts of the transition energy and its dependence on temperature, pressure, and external fields.

Isotope effects in the absorption and emission spectra of nickel-doped CdS and ZnS have been reported by us at the 1981 and 1984 International Conferences on luminescence.[23,24] Figure 7 shows the polarized spectra of a CdS crystal containing the nickel isotopes ^{58,60}Ni and ^{64}Ni in small but equal concentrations. The striking effect is that all the lines O_1,O_2,S_1,S_2, and E_1,E_2 in Fig. 2 are split into doublets, with a separation of 6Δ between the isotopes with mass 64 and 58; there is an isotope shift to shorter wavelengths with increasing mass and an average value of the isotope splitting of $\Delta=22$ μeV. Though for
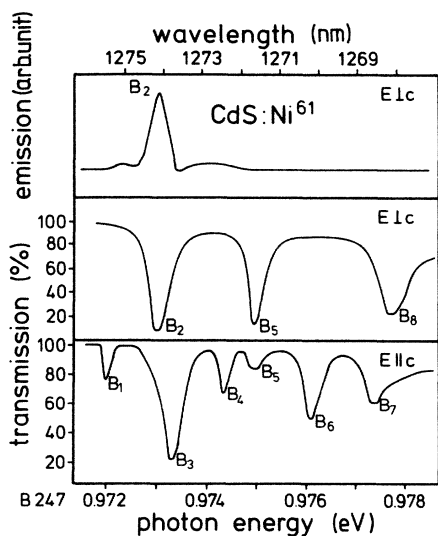

FIG. 6. Polarized emission and transmission spectra of a CdS crystal heavily doped with ^{61}Ni in the infrared spectral region $^3T_1(F)\leftrightarrow{}^3A_2(F)$ transition. Light source for emission: Ar-line$=488$ nm ($T=1.8$ K).
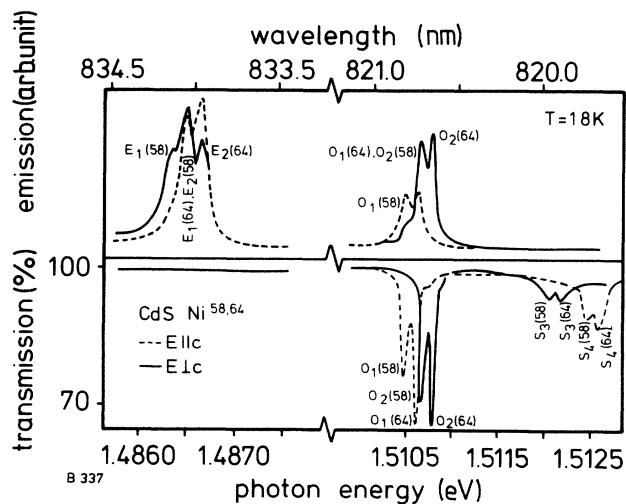

FIG. 7. Polarized emission and transmission spectra of a CdS crystal, weakly doped with $^{58/60}$Ni and ^{64}Ni ions. Isotope splittings are clearly visible.
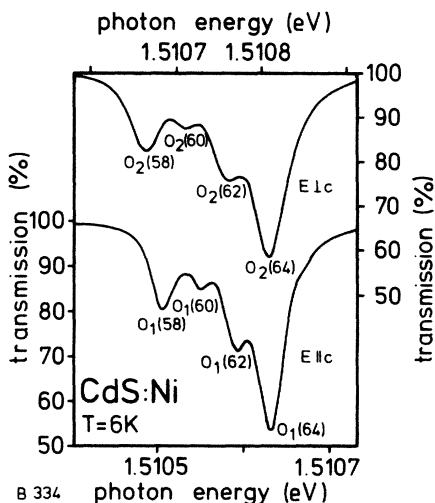
FIG. 8. Polarized transmission spectra of a weakly doped CdS crystal, containing the nickel isotopes ^{58}Ni, ^{60}Ni, ^{62}Ni, and ^{64}Ni. The scale on the left is valid for $\mathbf{E}||\mathbf{c}$, on the right for $\mathbf{E}\perp\mathbf{c}$.
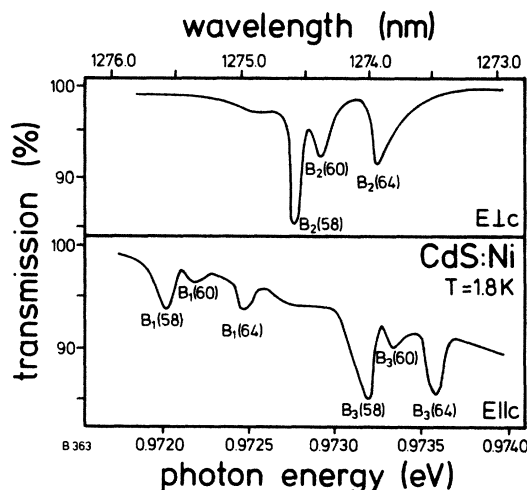

FIG. 9. Polarized infrared transmission spectra [$^{3}T_1(F)\rightarrow^{3}A_2(F)$ transition] of a medium doped CdS crystal, containing the Ni isotopes ^{58}Ni, ^{60}Ni, ^{64}Ni.

each doublet this value deviates slightly, and though Δ varies a little from specimen to specimen, no clear tendency may be detected from these measurements for any change of Δ with isotopic mass, polarization, or a particular transition. A 10% effect is just the limit of the measuring accuracy; this, however, is not due to the accuracy of optical apparatus, but, as we will see later, the isotopic shift Δ depends markedly on inner and outer conditions. As an example, we reproduce in Fig. 8 a transmission spectrum with four nickel isotopes for $\mathbf{E}||\mathbf{c}$ and $\mathbf{E}\perp\mathbf{c}$ polarization. In this particular case there is a medium isotope shift between ^{58}Ni and ^{64}Ni of 21 μeV for $\mathbf{E}||\mathbf{c}$ and 23 μeV for $\mathbf{E}\perp\mathbf{c}$, hence a difference of about 10%.

As for some other crystals (compare Figs. 11—13) where no such difference can be detected, one might guess that, for example, stress produced during the cooling procedure of the glued specimen may explain this effect.

New experiments of the isotope effect for the infrared $^{3}T_1(F)\leftrightarrow^{3}A_2(F)$ transitions, however, demonstrate the opposite. In Fig. 9 the transmission and emission spectra of CdS doped with ^{58,60}Ni and ^{64}Ni in the spectral region of about 1.273—1.275 μm are reproduced. A giant isotope effect becomes visible, about four times as big as for the $^{3}T_1(F)\leftrightarrow^{3}T_1(P)$ transitions. For the two opposite polarizations, however, an easily measurable difference exists of about 18% ($\Delta=83$ μeV, $\Delta=68$ μeV) for the transitions
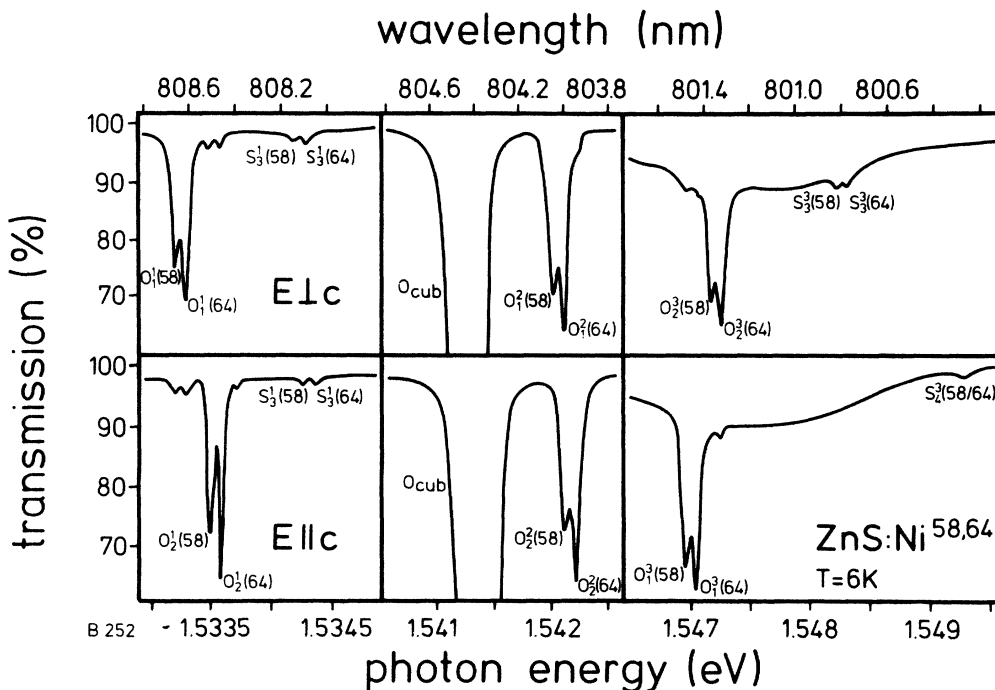

FIG. 10. Polarized transmission spectra of a weakly doped ZnS-polytypic crystal, containing the nickel isotopes ^{58}Ni, ^{60}Ni, ^{64}Ni.

TABLE I. Coupling constants and isotope shifts of the spectral lines and energy levels of the $^3T_1(F)\leftrightarrow{}^3T_1(P)$ and $^3T_1(F)\leftrightarrow{}^3A_2(F)$ transitions in CdS:Ni^{2+}. The coupling constant β_G of the ground state and D_∞^{61} can be taken from the values of B_2 to be 35.24. The values in this table are given in meV.

Observed fine structure line	Polarization	Δ_{62}^{61}	β_G-β_j	Δ_∞^{61}	β_j	D_∞^{61}
O_1	$E\|\|c$	0.021	9.02	1.31	26.22	3.81
O_2	$E\perp c$	0.023	9.88	1.44	25.36	3.69
S_3	$E\perp c$	0.020	8.59	1.25	26.65	3.87
S_4	$E\|\|c$	0.021	9.02	1.31	26.22	3.81
B_1	$E\|\|c$	0.077	33.09	4.81	2.15	0.31
B_2	$E\perp c$	0.082	35.24	5.12	0	0
B_3	$E\|\|c$	0.069	29.65	4.31	5.55	0.81

B_2, B_3, and of 10% for the low-energy group (B_7,B_6) not shown here (Fig. 6). The energy difference between the transitions B_2 and B_3 decreases for increasing isotope mass. Thus for hypothetical nonvibrating Ni atoms with infinitely big mass the electronic splitting under the influence of the trigonal field tends to zero or even to the opposite sign.

Isotope splittings for the $^3T_1(F)\rightarrow{}^3T_1(P)$ transition have been detected also in ZnS-Ni crystals.[24] For a crystal weakly doped with $^{58/60}$Ni and ^{64}Ni the transmission spectrum is given in Fig. 10. The highly resolved spectra show in most cases a doublet structure, from which an isotope splitting of $\Delta=18\pm1$ μeV can be deduced. Within the accuracy of our measurements, no deviation from this value for the different groups of transitions could be detected. Isotope effects in the emission spectra and for the $^3T_1(F)\rightarrow{}^3A_2(F)$ transition have up to now not been investigated. Our experimental results for all isotope splittings Δ of CdS are compiled in Table I.

D. Dependence of the isotope splitting on temperature, stress, and magnetic field

In the preceding section we studied the variation of the isotope effect of Ni atoms in different environments, tran-
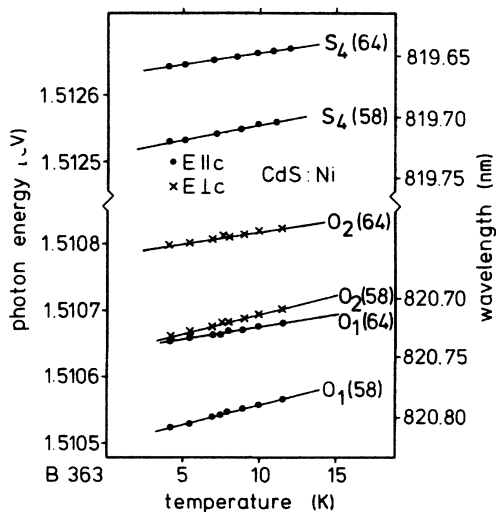
sitions and polarizations. Marked, but stepwise changes could be reported. It is obvious that changes of the isotope splittings should be expected for a variety of influences, which alter the vibration frequencies of the lattice, and of the impurities by changing the spring constants between the impurity and its surroundings. Temperature, pressure, and applied electric and magnetic fields are such influences. They allow the continuous observation of the change of the splitting energy of different isotopes for the same specimen.

The energy position of the lines O_1, O_2, and S_4 for a CdS crystal doped with $^{58/60}$Ni and ^{64}Ni is given in Fig. 11 for different temperatures. From this the temperature dependence of the isotope splitting can be drawn. With increasing temperature one observes an increase of the energy for all lines. For different isotopes the slope of the curves is the steeper, the lighter the mass is: the isotope splitting decreases in a measurable and reproducible way, and reaches a loss of about 10% even for the relatively small temperature interval, shown here. Unfortunately, the zero-phonon lines vanish at still higher temperatures so that their shifts cannot be followed any further. It can be imagined that with further increasing masses of the impurity, finally a temperature dependence would follow being entirely different from that observed here.

A similar observation has been made by applying uniaxial stress to the crystal. We will report on the details of such experiments in a separate paper.[25] Here only the behavior of the isotope splitting for one single geometric arrangement will be described. In Fig. 12 the stress dependence of the lines O_1 and O_2 for ^{58}Ni and ^{64}Ni for

FIG. 11. Temperature dependence of zero-phonon transition lines O_1, O_2, and S_4 of a CdS crystal for nickel isotopes ^{58}Ni and ^{64}Ni.
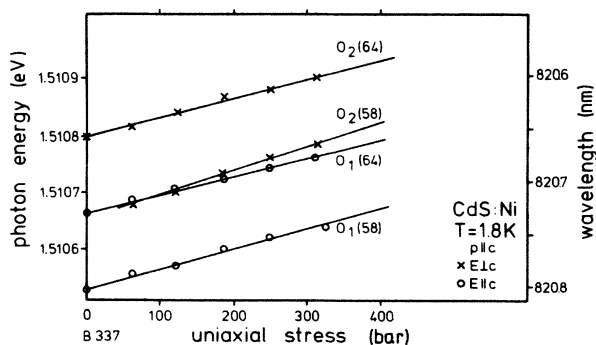
FIG. 12. Pressure dependence of zero-phonon transition lines O_1, O_2 of a CdS crystal for nickel isotopes ^{58}Ni and ^{64}Ni.
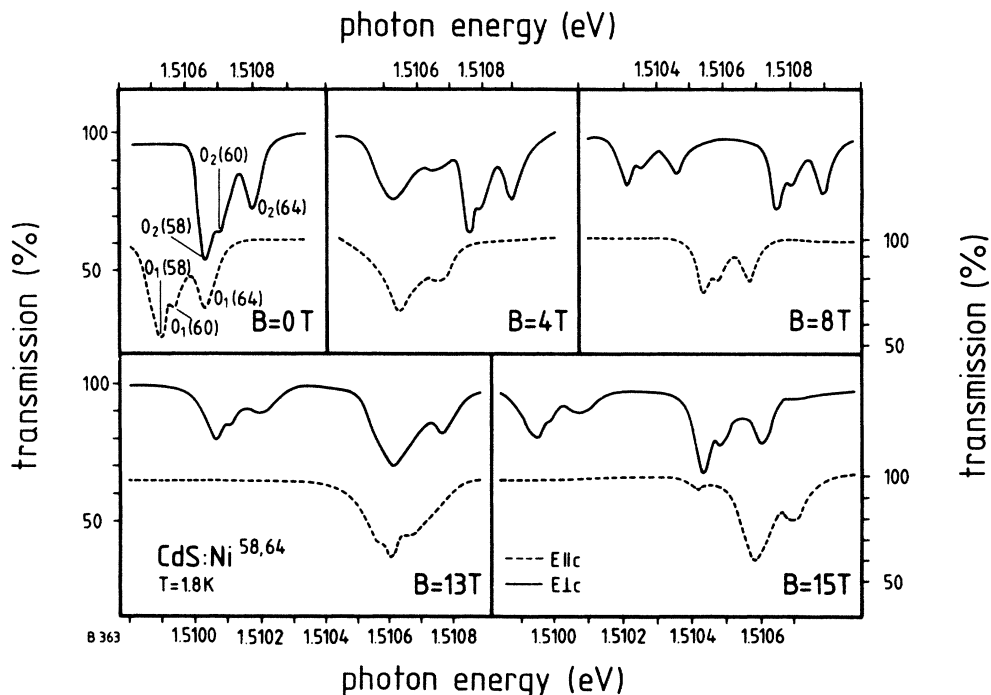
FIG. 13. Transmission spectra of a weakly doped CdS crystal containing the nickel isotopes $^{58/60}$Ni and ^{64}Ni for different magnetic field strengths. Left scale valid for $E\perp c$, right scale for $E||c$.

p||c and $E||$,$\perp$c is given. While for one isotopic weight the lines O_1 and O_2 tend to show a higher separation, the opposite is true for Δ^{58}_{64}: A decrease of about 10% can easily be detected for a stress of $p = 300$ bar, a value, which is still relatively small. Again we find for a further increase of the mass value, the slope of the stress dependence would be changed entirely. Again it becomes obvious that the small isotope effect can cause macroscopic effects, which cannot be understood without including vibronic effects.

Finally we give more details on the effect of a magnetic field to the isotope splitting, reported earlier by us.[23] In Fig. 13 the spectra of a crystal containing $^{58/60}$Ni and ^{64}Ni are reproduced for different magnetic fields H||c. As can clearly be seen, a very pronounced effect occurs. For $E\perp c$ the two magnet-field split triplets O_2 show an entirely

different behavior: The isotope-split doublet with the higher energy has at 15 T a splitting constant 30% higher than without a magnetic field, while the triplet with the lower energy shows no measurable change. The same is true for the line O_1, which does not split and which shifts only very little with magnetic field. The full magnetic field dependence for other spatial configurations is shown in Fig. 14. The complicated Zeeman pattern gives an impression of the complexity of this problem. These experiments show that the isotope effect creates difficulties in the understanding of the normal Zeeman effect. Depending on the isotope weight, the shape of the curves is entirely changed. To determine g values the electron-phonon coupling must be taken into account.

E. Energy transfer process between different Ni centers

The above described observations, that the linewidth of zero-phonon lines in the nickel 3d absorption and emission depends strongly on the impurity concentration, show clearly that interactions between neighboring nickel centers occur. The fact, that for concentrations smaller than 0.01 ppm measurable effects still occur, demonstrates that the medium distance for such interactions is of the order of magnitude of several tens of nm, a value which is too large to be explained by local lattice deformation. Therefore energy transfer is the most probable process. The existence of isotope effects creates the possibility of studying energy transfer processes in a unique way. By exciting one particular nickel isotope the intensity and time delay of the radiative transitions at another nickel isotope can be studied. In addition, level crossing experiments become possible, if through the action of outer in-
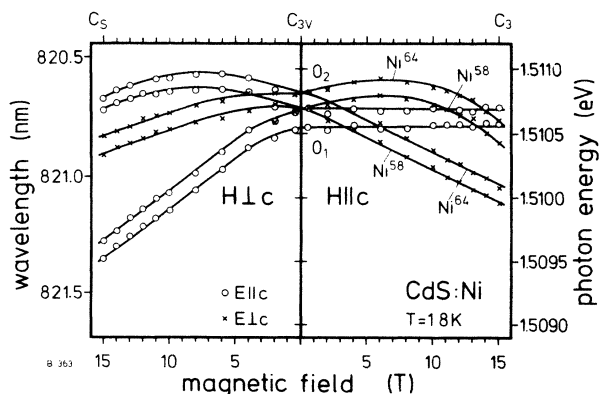

FIG. 14. Zeeman effect of the transmission minima $O_1,O_2(58)$ and $O_1,O_2(64)$ for a weakly doped CdS crystal. Its spectra are shown in Fig. 12.
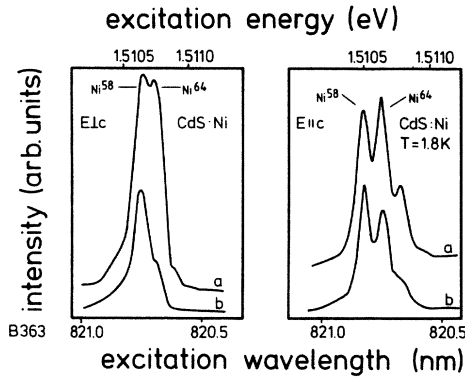
FIG. 15. Polarized excitation spectra of the E lines (Fig. 7) for light absorbed in the region of 0 lines for different nickel isotopes. (a) Emission observed at $^{64}E_1$ and (b) emission observed at $^{58}E_1$.

fluences energy levels of different polarization can be shifted, so that different isotopes show equal energy states. In the following we present two examples of such effects for the $^3T_1(F)\leftrightarrow^3T_1(P)$ transition in CdS. They are, however, still of a preliminary character.

By repeating the excitation experiment of Fig. 4(b) with much higher resolution it became possible to compare the excitation probability for the E lines for the ^{64}Ni and $^{58/60}$Ni isotopes, respectively, if light was absorbed in the region of the 0 lines (Fig. 15). The main result is, as expected, the occurrence of two apparently different excitation spectra. However, it is still possible to observe that absorption in a ^{64}Ni ion can excite the $^{58/60}$Ni centers and vice versa. It is also obvious, that the energy transfer from the $^{58/60}$Ni excitation to the ^{64}Ni emission is markedly lower than in the opposite case, a consequence of the fact, that energy can be shifted more easily from higher- to lower-lying levels. Further experiments with such a system, including transient effects, might help us to understand the mechanism of energy transfer processes in II-VI compounds doped with transition elements such as Ni in more detail.

The second experiment can be discussed with the help of the spectra of Figs. 13 and 14. When increasing the magnetic field it occurs two times, that the $^{58/60}$Ni-line polarized $E\perp c$ crosses the $^{58/60}$Ni line for $E||c$. At these magnetic fields (3, 5, and 13 T) a sudden broadening of lines occurs, instead of a triplet, only a doublet can be resolved. In other words, through the level crossing for a particular isotope at different polarizations it becomes possible to get absorption between two neighboring isotope lines, where normally it is only a weak absorption in that particular polarization. It is likely that a spin-spin exchange interaction between different isotopes occurs at the level crossing, so that a depolarization effect becomes effective. Further experiments are necessary to elucidate this interesting effect, which might also be of importance for problems of semimagnetic semiconductors of the $Cd_xNi_{1-x}S$ type.

III. DISCUSSION

The experimental results described above, have added new, important, and very precise information to our knowledge of the optical properties of CdS and ZnS crystals doped with nickel impurities. First, it has become absolutely clear that the static crystal field theory is unable to explain this work's fine-structure spectra. Isotope splittings are definitely connected with lattice vibrations but these are not included in such theories. In addition, as mentioned already by Kaufmann and Koidle[5,6] (KK) for the case of nickel in ZnS, the symmetries of the zero-phonon lines are according to those expected when assuming a Ni^{2+} impurity in a static lattice. Second, due to the achieved high-resolution explanations, earlier results may be tested in which the coupling of electronic and phononic states has been hypothetically discussed. As a consequence of observing the highly resolved optical properties for different transitions, chemical components, and crystal symmetries, as well as under the action of changing temperature, pressure, and magnetic field, we found it obvious that none of the existing theories is able to explain our main results. In the following a more comprehensive model is discussed qualitatively—the quantitative theory is given by Nestler and Scherz[26] elsewhere.

In Fig. 3 the level scheme of a Ni^{2+} ion in a tetrahedral environment is reproduced. In contrast to the usual static model the influence of phonons and their interaction with the electronic states is included. As the trigonal crystal fields only have relatively small influence, we have included them in the last place.

First, we assume that different local phonons couple to the particular energy levels of the crystal field and spin-orbit split-energy system in the usual way. A ladder starting with the zero-point energy exists and has to be considered for quantitative arguments up to quantum number $n \sim 10$; only the first ($n = 1$) term and only for the E,T_2 level of the ^3P state and of the T_2 term of the ^3F state, is shown in our scheme. Further, we assume that the local phonon energy exceeds that of the lattice phonons by a certain amount which seems to be necessary to explain the existence of strong Jahn-Teller couplings shown in the fifth column of Fig. 3. This coupling can principally occur with several of the vibrational modes of the Ni^{2+}-S_4 tetrahedron, however, several arguments[26,27] exist that regard mainly the T_2 modes. While this is very important for a quantitative theory, for our qualitative picture it is not that relevant.

Jahn-Teller coupling, as is known, splits and reduces the phonon energy considerably and produces additional lines with partly zero-phonon character. It is commonly assumed that the coupling is different for the different electronic terms,[28,29] so that the final line structure has lost any similarity to the static model. In order to understand isotope splittings it has also been argued that the local phonon frequency should be different for different excited states of the same impurity.[29,30] It will be shown that both assumptions must be considered simultaneously to understand our results.

A. Level structures

We first discuss the line structure of the near-infrared region due to the $^3T_1(P)\leftrightarrow^3T_1(F)$ transitions in the two sulfur compounds of Zn and Cd. For cubic ZnS, Kauf-

mann and Koidle[5,6] (KK) describe their results—a strong zero-phonon line at $h\nu = 12\,436$ cm^{-1}, a weak nonpolarized line, 6 cm^{-1} shifted to higher energies and a very weak line shifted 14 cm^{-1} further by assuming an allowed crystal-field transition between the A_1 level of the $^3T_1(F)$ term and the T_2 level of the $^3T_1(P)$ term, a dipole-forbidden transition to the E level of the $^3T_1(P)$ term and a vibronic A_1 level; the latter existing due to a Jahn-Teller coupling of the T and E modes of an acoustical LA-phonon with the mentioned electronic E level. This picture was apparently confirmed by Zeeman's experiments[31] showing a threefold splitting of the strong cubic line and a doublet arising from the forbidden transition to the E level. While our experiments (Fig. 2) with two cubic-polytypic ZnS crystals principally confirm the spectral positions of the three lines, important differences exist, which make their interpretations doubtful. First, a doublet structure for $E\|c$ and $E\bot c$ could clearly be resolved for the lines O_1^2, O_2^2 with an order of magnitude comparable to the splitting of the 0 lines in hexagonal CdS (Fig. 1). But trigonal field, arising, for example, from the polytypic structure of our crystal cannot split a Kramers-forbidden E term. Second, for more than 50 crystals we found the two additional doublets $O_1^{1,3}, O_2^{1,3}$ to be always identical transmission intensities as O_1^2, O_2^2, independent of the transmission value of the cubic 0 line. This makes it more probable, that also the $O_{1,2}^2$ doublets are of similar structure to the two others. Indeed, new Zeeman experiments have resulted in a threefold splitting of this level, which could not be explained if one relates it like KK[5,6] to an E term. Finally, from the spectrum of the highly doped crystal in Fig. 2 it becomes clear that in addition to the 0 lines in all three cases, two lines with higher energies follow.

The explanation for all this seems simple now. The cubic line is indeed caused by an allowed transition to the T_2 level and there is for cubic ZnS no other zero-phonon line involved. This line indeed splits by a magnetic field into three sublevels. The remaining structures come from three different axial symmetric environments of Ni in polytypic ZnS, they are linked to each other in our particular crystals in equal amounts. Their structures can be understood in the same way as has been done already for the hexagonal CdS-Ni lines. The two differently polarized O_i lines are due to transitions into (or from) the T_2 level, split by a trigonal crystal field into an A_1 and an E level, while the weak lines are caused by transitions into the electronic E level and an A_1 term, deduced, as discussed, from the phonon component, distorted by the Jahn-Teller effect. Their polarization and magnetic-field dependence is in good agreement for such an assumption.

Due to our model, further phononlike components at still higher energies are to be expected. In fact for CdS-Ni such lines can be seen (Fig. 1). They are somewhat more broadened than the four lines, discussed up to now, and are thus relatively weak.

There remains to understand the radiative transitions E_i at lower energies than O_i, for which in no case could a corresponding absorption be found. In contrast to earlier assumptions, the lines can now be explained best by a transition from the $^3T_1(P)$ term to excited terms of the

$^3T_1(F)$ level (Fig. 3). Since at low temperature these levels are not occupied, absorption cannot be expected. It is important to note that for CdS and all four symmetries of ZnS with only small deviations, almost the same shift against the transition energy to the ground A_1 level exists (Figs. 4 and 5). For higher doped ZnS crystals, the level structure of the absorption spectrum is repeated, in emission, however, with dramatically changed intensity ratios, since now the transitions also in the cubic case are no longer dipole forbidden. This confirms additionally, we believe, our level scheme.

The second spectral region investigated here only for CdS concerns the line group B_i around 1.25 μm. From the literature[32] it is obvious, that a transition within the ^3F level is involved, starting or ending at the highest $^3A_2$ level. In emission again, two groups of lines can be observed, with exactly the same difference as in the case of the $^3T_1(F) \rightarrow ^3T_1(P)$ lines for the lines O_i and E_i. This shows clearly that the same excited states of the $^3T_1(F)$ level are involved. Similar observations have been published also for ZnS-Ni crystals. A detailed discussion of the spectra and the energy structure of these transitions will be given elsewhere.[24] Here we mention only that the lines B_1 and B_2 correspond to the lines O_1 and O_2 for the $^3T_1(F) \leftrightarrow ^3T_1(P)$ transitions, while B_3 has to be compared with the S_4 line. These transitions have their importance for the explanation of the isotope effect discussed in the following section.

B. Isotope effect

A quantitative theory, which would allow us to present our energy model in absolute energy values, immediately should result in the determination of the correct isotope splittings. Different masses of nickel atoms give rise to different vibrational energies, thus changing the energy of the optical transition in a definite way. Furthermore, all other influences, which change phonon energies and electron-phonon coupling, should cause changes of the positions of the levels. There is, however, one additional assumption of basic importance. In order to avoid the isotope splitting being zero we have to assume, like other authors,[28,30] that the two involved levels of a particular transition couple to different phonon ladders. Using in addition the concept of the Jahn-Teller distortion, indeed, it is the energy difference of the shifts shown in Fig. 15, which gives the isotope splitting. Naturally, then, different types of transitions may result in different isotope splittings, as has been shown for CdS-Ni^{2+} in this paper for the first time. Fortunately, the two transitions have in common the A_1 ground state of the system, and only the excited states differ. As one of these states, a $^3A_2(F)$ state, can be shown in first order to be a resonant gap mode and thus has phonon frequencies independent of the impurity mass. The isotope splitting of the ground state can be determined, and from this also, the absolute values of the shifts of the excited $^3T_1(P)$ levels.

In a crude approximation our model can be put in a numerical form, if we assume that the energy of the phonons $\hbar\omega_i$ belonging to the ith level giving rise to the shift in the 4th column of Fig. 3 can be expressed by the masses of

the vibrating nickel ion (M) and its sulfur neighbors (m), a spring constant k_i and a mass independent additive term k_e^0 by (lower case)

$$\hbar\omega_i = k_i[3 + (m/M)]^{1/2} + k_e^0 \ . \tag{1}$$

This formula is somewhat similar to that given by Imbusch et al.[30] and has been developed by Nestler[27] to include not only the five particle cluster Ni^{2+}-S_4, but also its imbedding in an infinitely big crystal. The spring constant k_i and the constant k_e^0 are then, as mentioned, in principle different for different energy levels of the impurity ion. The $^3T_1(F)$ levels hold probably $k_e^0 \ll k_i$, while for the gap modes at the $^3A_2(F)$ level the opposite will be true.

Of an even more qualitative character is the additional assumption that the energy shift by electron-phonon interaction, as seen in the 5th column of Fig. 3, is proportional to the phonon energy with the proportionality factor α being independent of M:

$$\Delta E = \alpha_i \hbar\omega_i \ . \tag{2}$$

The coupling constant will be different for the different split levels arising from one degenerate energy plateau and also from different levels. For a particular transition between two levels i and j an isotope splitting constant Δ between the masses M and $M+1$ can then be calculated according to

$$\Delta = (\beta_i - \beta_j)\{(3 + m/M)^{1/2} - [3 + m/(M+1)]^{1/2}\} \tag{3}$$

with

$$\beta_i = \alpha_i k_i; \quad \beta_j = \alpha_j k_j \ .$$

For the two principal transitions discussed in this paper, we receive by inserting the measured Δ values given into Eq. (3) the mean values for the coupling constants $\beta_i - \beta_j$ (Table I). From this the shift Δ_∞^{61} of the lines from a hypothetical nonvibrating nickel isotope $(M \rightarrow \infty)$ to the existing isotope $M = 61$ can be calculated. Values in the order of magnitude 1 meV are found.

To determine the corresponding isotope shifts of each of the involved energy levels, given by the $\beta_{i,j}$, we need additional information. Unfortunately the luminescence transitions $^3T_1(P) \rightarrow ^3A_2(F)$ could not yet be observed, as it is expected in the infrared spectral region around 2.2 μm, where our experimental setup did not work. There exist, however, as mentioned in theoretical arguments, that the isotopic shift of the $^3A_2(F)$ level by the electron-phonon interaction should be much smaller than for other representations. In a first approximation we assume therefore that the E term of the $^3A_2(F)$ level does not change at all with the isotope weight, i.e., its β is at zero. Then, indeed, all the other β values and the isotope shifts D_∞^{61} of the levels from $M = \infty$ to $M = 61$ can be calculated. Values up to 6 meV result (Table I). They are big compared with the splitting energy of the trigonal crystal field and at least an order of magnitude larger than shifts and splittings by stress, temperature, or magnetic fields. From this it becomes quite clear, that neglecting of vibra-

tional effects in the discussed system can never lead to an understanding of the experimental details. Furthermore, it is obvious, that isotope shifts of spectral lines are normally much smaller than the corresponding shifts of the energy levels: only the differences become observable. If, however, one of the involved levels show only a small effect, giant isotope splittings occur.

Equation (3) can be used as a basis to understand most of our observations at least in a qualitative way. The comparison of the isotopic shift for CdS-Ni^{2+} and ZnS-Ni^{2+} confirms the validity of our basic assumption to discuss the vibronic effects in terms of a Ni^{2+}-S_4 cluster. Only the second nearest neighbors are then different for the two compounds and this will not alter the spring constant very much. But in any case, the k_i in Eq. (1) will be smaller the lower the atomic weight of the anion is. The relative small difference of about 10% can thus be understood easily.

The observed difference of the isotope splitting constant for the lines polarized $E\|c$ or $E\perp c$ is also understandable from Eq. (3). There will be both a change of phonon frequency (k_i) and electron-phonon interaction with the change of the polarization vector, if one excites a vibration in the cluster imbedded in a hexagonal crystal. Since in the literature the frequency shift seems to be small for phonons traveling parallel or perpendicular to the c axis, indeed, only small effects are observed.

As a result of the special form of the mass dependence, the splitting constant Δ should be slightly different for different isotopes. The difference Δ_{60}^{58}, for example, must differ from Δ_{64}^{62} for the $^3T_1(F) \rightarrow ^3T_1(P)$ transition by about 12%. From a very precise analysis with a CdS crystal containing 4 nickel isotopes (Fig. 6), indeed, a change in such order of magnitude is indicated, but further, very precise experiments should be performed to clear this question.

Uniaxial stress is known to alter phonon frequencies considerably. At the same time the electron-phonon interaction will also be affected. In the framework of our qualitative theory it becomes quite simple then to understand the results presented in Fig. 12. For a pressure of 400 bar we observe a change of Δ of about -10%. This can be explained by a reduction of $\beta_i - \beta_j$ in Eq. (3) also by about 10%. As a result the shift of each line due to pressure should then also be 10% of Δ_∞^{61} which is about 140 μeV in very good coincidence with the observed value.

The validity of Eq. (3) is confirmed also by our temperature-dependent experiments. From the direction of the shift and a comparison with the stress-affected dilatation one would expect a shrinking of the crystal rather than an expansion with temperature. Indeed, for temperatures under 50 K hexagonal crystals of the CdS type show an anomalous[33] behavior, the coefficient of expansion is negative.

It remains to discuss the effect of a magnetic field. In this case, a strong change of the electronic configuration results and this will definitely change the electron-phonon interaction. For $H\|c$, $E\perp c$ a huge change of Δ of the order of 25% results at 15 T. There it is quite obvious, that the normal Zeeman behavior of a pure electronic system is

entirely changed, the lines bend back to lower energy by about 2 meV, which is not so far from the expected value. To understand all the details completely, a comprehensive theoretical treatment is necessary which will be dealt with elsewhere.

To conclude, the effect of electron-phonon coupling has been clearly demonstrated to be valid for the different observed phenomena. At least for the nickel in CdS and ZnS system all observed optical properties are strongly isotope mass dependent and a simple crystal-field model fails in any respect. Our qualitative energy model, however, is not able to give quantitative explanations. Detailed calculations have been already published[34] and further theoretical considerations are under progress.

ACKNOWLEDGMENTS

[1]H. A. Weakliem, J. Chem. Phys. 36, 2117 (1962).

[2]R. Pappalardo and R. E. Dietz, Phys. Rev. 123, 1188 (1961).

[3]M. L. Reynolds, W. E. Hangston, and G. F. J. Garlick, J. Phys. C 2, 361 (1969).

[4]I. Broser, R. Germer, H. J. Schulz, Phys. Status Solidi B 101, 181 (1980).

[5]U. G. Kaufmann, P. Koidl, and O. F. Schirmer, J. Phys. C 6, 310 (1973).

[6]U. G. Kaufmann and P. Koidl, J. Phys. C 7, 791 (1974).

[7]U. Kaufmann, W. H. Koschel, J. Schneider, and J. Weber, Phys. Rev. 19, 3343 (1979).

[8]G. Roussos, Ph.D. thesis, Technische Universität Berlin, 1983.

[9]G. Roussos and H. J. Schulz, Solid State Commun. 51, 663 (1984).

[10]D. Buhmann, H. J. Schulz, and M. Thiede, Phys. Rev. 24, 6221 (1981).

[11]S. G. Bishop, D. J. Robbins, and P. J. Dean, Solid State Commun. 33, 119 (1980).

[12]I. Broser, A. Hoffmann, and R. Broser, in Proceedings of the 4th Lund International Conference on Deep Level Impurity in Semiconductors, Eger, Hungary, 1984 (unpublished).

[13]H. A. Jahn and E. Teller, Proc. R. Soc. London, Ser. A 161, 220 (1937).

[14]F. S. Ham, Phys. Rev. 138, A1727 (1965).

[15]M. D. Sturge, Solid State Phys. 20, 91 (1967).

[16]R. Frerich, Naturwiss. 33, 281 (1946); I. Broser and R. Broser-Warminsky, Deutsches Patentamt, Patentschrift Nr. 814 193 (1950).

[17]R. Broser, G. Hildebrandt, and H. Reibedanz, Phys. Status Solidi A 14, K11 (1972).

[18]I. Broser, R. Germer, and H. J. Schulz, Phys. Status Solidi B 101, 181 (1980).

[19]A. Schröder, Diplomarbeit, Technische Universität Berlin, 1981.

[20]B. Nestler and U. Scherz, J. Lumin. 24/25, 229 (1981).

[21]I. Broser, R. Germer, F. Seliger, and H. J. Schulz, Phys. Chem. Solids 41, 101 (1980).

[22]R. Germer, Phys. Rev. B 27, 2412 (1983).

[23]I. Broser, R. Germer, A. Schröder, E. Birkicht, and R. Broser, J. Lumin. 24/25, 225 (1981).

[24]I. Broser, R. Broser, E. Birkicht, and A. Hoffmann, J. Lumin. 31/32, 424 (1984).

[25]I. Broser, A. Hoffmann, and H. Schuster (unpublished).

[26]B. Nestler and U. Scherz (unpublished).

[27]B. Nestler, Ph.D. thesis, Technische Universität Berlin, 1985.

[28]U. Heine and C. H. Henry, Phys. Rev. B 11, 3795 (1975).

[29]J. A. van Vechten, Phys. Rev. B 13, 946 (1976).

[30]G. F. Imbusch, W. M. Yen, A. L. Schawlow, G. E. Devlin, and J. P. Remeika, Phys. Rev. 136, A481 (1964).

[31]R. Germer, F. Seliger, U. Kaufmann, and J. Schneider, J. Phys. C 14, 2535 (1981).

[32]Y. P. Gnatenkho and A. Kh. Roszhko, Pis'ma Zh. Eksp. Teor. Fiz. 24, 125 (1976) [JETP Lett. 24, 107 (1976)].

[33]S. Browder and S. S. Ballard, J. Appl. Phys. 11, 841 (1972).

[34]B. Nestler, U. Scherz, A. Hoffmann, and I. Broser, in Proceedings of the 5th General Conference CMD of the EPS, Berlin, 1985 (unpublished).